

Opening Up the Next Chapter in Clinical Laboratories

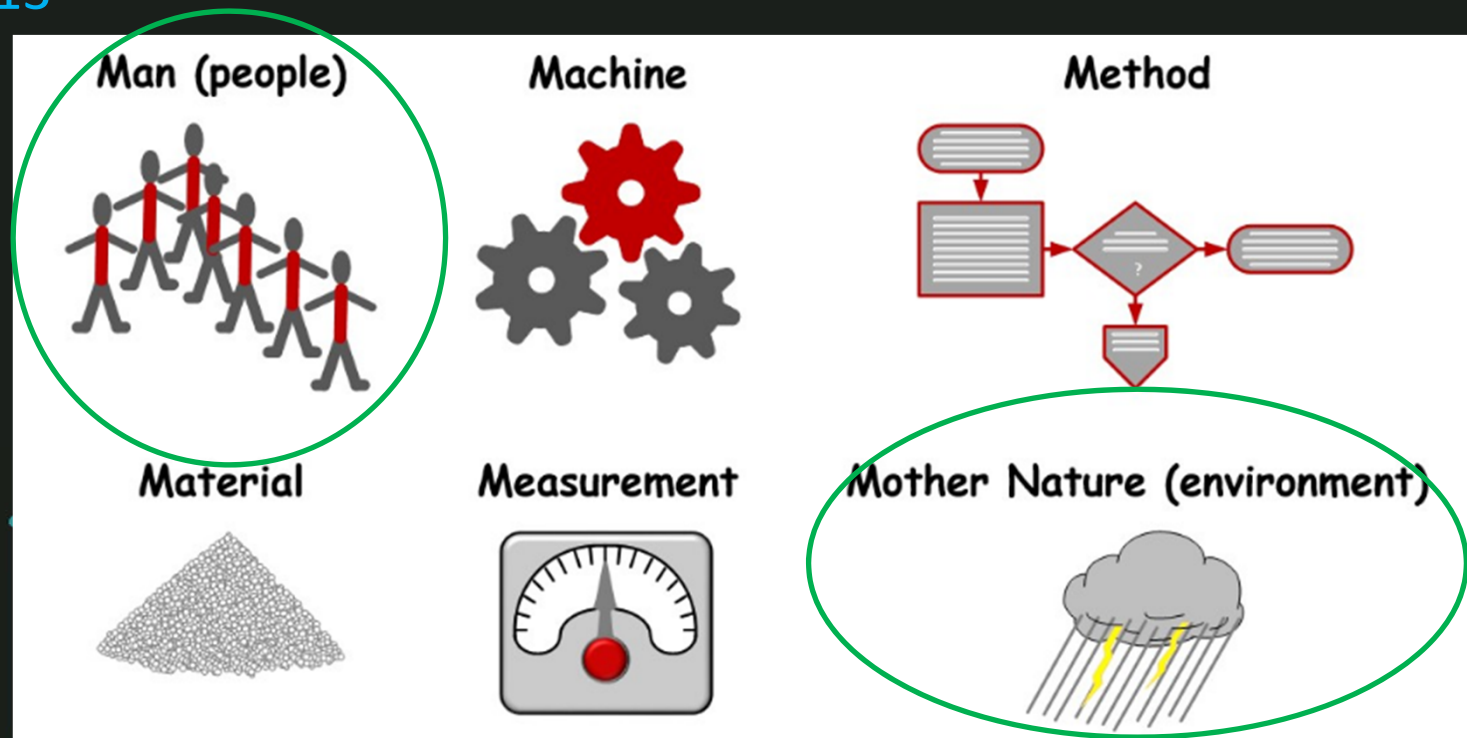
Dr Kristine Luk

KWC Service Director (Pathology)
Chief of Service (Pathology), PMH/NLTH

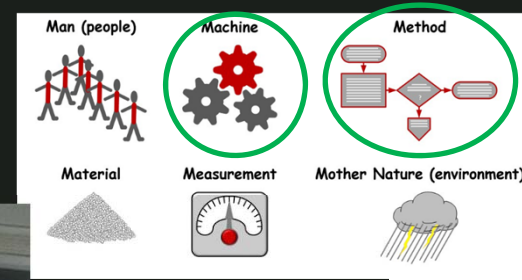


Guangdong second provincial people's hospital

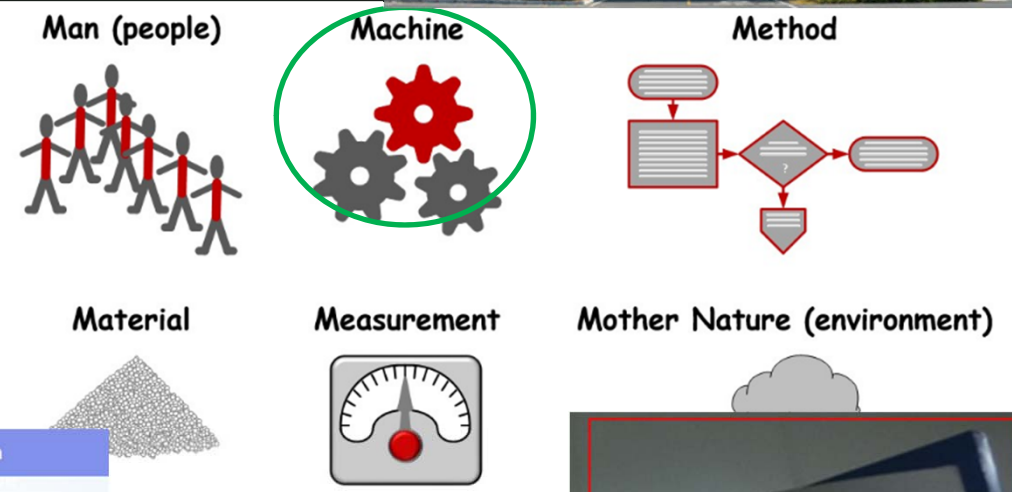
- 1730 beds
 - Total staff 3006, post-graduate qualification 935
 - master tutors 107
 - PHD tutors 13
 - A Biosafety Level 3 laboratory
 - >2000m³ medical laboratory
 - >1000 m³ animal laboratory
- Research and publications, patent application as important resources for hospitals



Automation & paperless workflow - from specimen collection to reporting, storage & QC



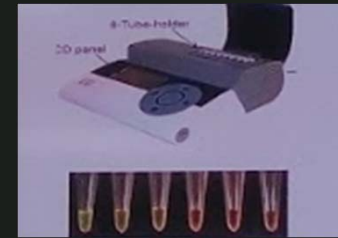
Financial initiatives to evaluate new machines from industries



Category	Product Name	Target Pathogen
Respiratory Infections	Respiratory 7 Types Pathogen Multiplex Nucleic Acid Detection Kit	FluA, FluB, RSV, ADV, HRV, HPIV and MP
	Respiratory 8 Types Pathogen Multiplex Nucleic Acid Detection Kit	FluA, FluB, RSV, ADV, HRV, HPIV, MP and SARS-CoV-2
	Respiratory 17 Types Pathogen Multiplex Nucleic Acid Detection Kit	FluA, FluA/H1, FluA/H3, FluB, RSV, ADV, HRV, HPIV1, HPIV2/4, HPIV3, CP, MP, CorHKU1/OC43, CorNL63/229, HMPV, HBoV and SARS-CoV-2
Gastrointestinal Infections	Gastrointestinal Bacteria Virulence Gene Nucleic Acid Detection Kit	21 types of common gastrointestinal bacteria virulence genes including ipaH, cdtA, aggR, eae, O1rfb, ompW, cdtB, stx2, SENI383, invA, cdtC, ETEC-lt, tli, O139rfb, ctxA, foxA, stib, stxI, STY4669, STM0159
Sexually Transmitted Infections	Human Papilloma Virus (HPV) Multiplex Genotypes Nucleic Acid Detection Kit	18 types of HPV including 16, 18, 26, 31, 33, 35, 39, 45, 51, 52, 53, 56, 58, 59, 66, 68, 73 and 82
	Sexually Transmitted Infections Multiplex Nucleic Acid Detection Kit	9 types of STIs including CT, NG, UU, TV, MG, MH, UP, HSVI, HSVII



Point of Care of Tests (POCT)

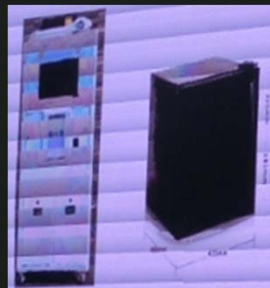


The Third People's Hospital of Shenzhen

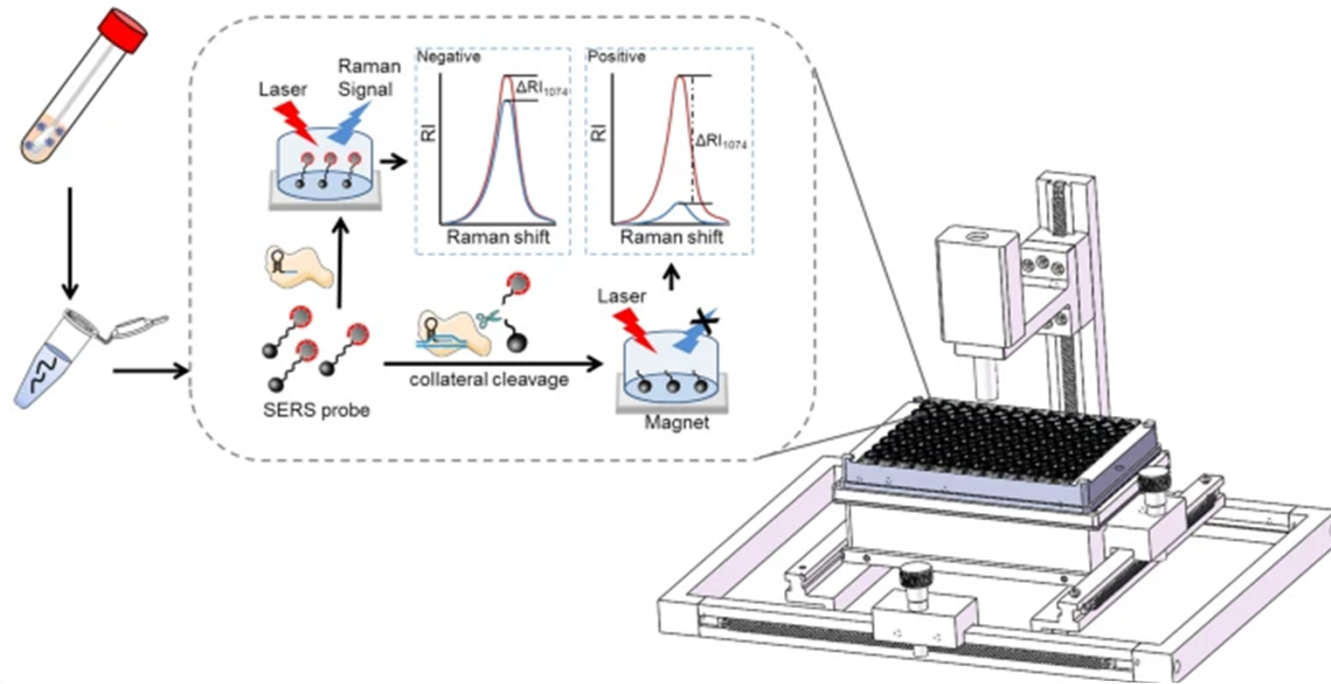
- Self-collection of respiratory specimens and full automation
- Multiplex PCR against 8 pathogens, including SARS-CoV2, *Mycoplasma pneumoniae*, influenza
- 30 minutes analytical time
- LOD 100 copies/mL

Emergency care for disasters/epidemics

- Gram stain and culture of blood and sterile body fluid
- CSF cell count and protein
- Procalcitonin and C reactive protein
- *HIV, syphilis serology, IL-6, bacterial antigen, Influenza A/B, rotavirus antigen/antibody, Influenza A, B, SARS-CoV2, Vibrio cholerae PCR*
- Loop-Mediated Isothermal Amplification (LAMP) <20 min
TB, DenV1-4, H7N9, *Legionella pneumophila, Salmonella*



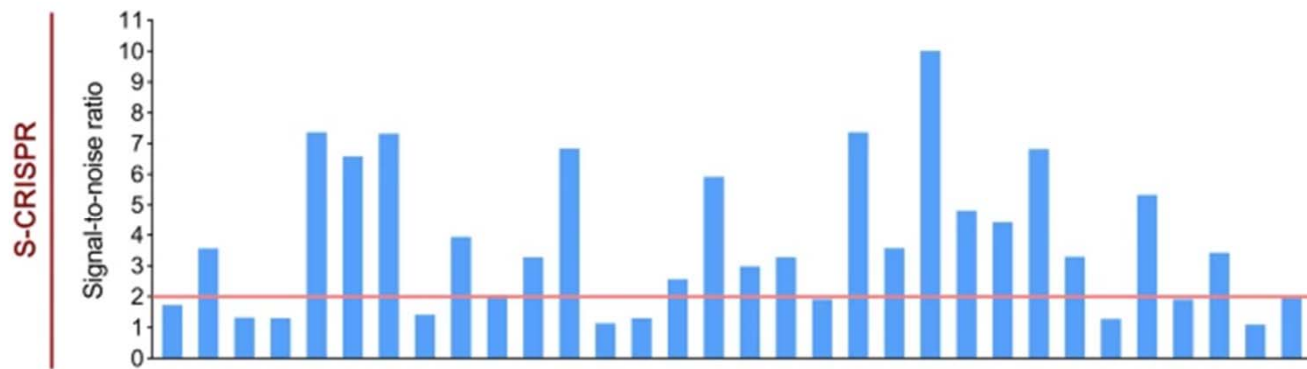
Amplification-free SERS-based CRISPR/Cas12a platform



- metallic nanoscopic surfaces generate Raman enhancement effect: surface-enhanced Raman scattering (SERS)
- Sensitivity 87.5% Specificity 100%
- 30-40 min
- <2 weeks to develop the probe

Liang et al. / Nanobiotechnol (2021) 19:273

b
PCR C_t 39 37 - - 24 32 31 39 34 39 37 29 - - 35 26 35 35 - 24 33 18 35 37 25 31 - 36 40 36 - -



Sample No.	1	2	3	4	5	6	7	8	9	10	11	12	13	14	15	16	17	18	19	20	21	22	23	24	25	26	27	28	29	30	31	32
PCR	+	+	-	-	+	+	+	+	+	+	+	+	-	-	+	+	+	+	-	+	+	+	+	+	+	+	+	-	+	+	-	-
S-CRISPR	-	+	-	-	+	+	+	-	+	+	+	+	-	-	+	+	+	+	-	+	+	+	+	+	+	+	-	+	-	+	-	-



Cutting edge technology

A multiplex PCR-dipstick

LOD 10 CFU/mL,
Sensitivity >95% Specificity 100%
>0.97 kappa correlation with DNA
sequencing
<2 hours

Canadian Journal of Infectious Diseases and Medical Microbiology
Volume 2023, Article ID 6654504, 7 pages

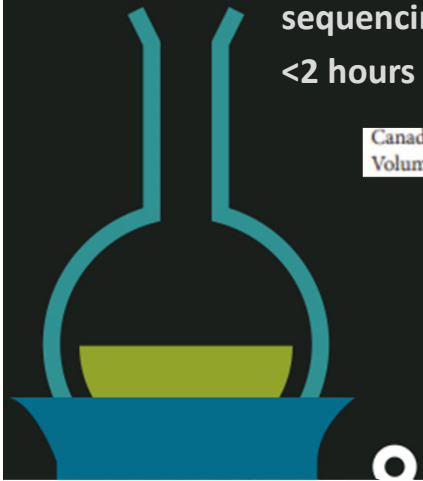


FIGURE 2: Specificity of multiplex PCR-dipstick chromatography. 1: negative control; 2: *M. pneumoniae*; 3: *C. pneumoniae*; 4: joint detection of *M. pneumoniae* and *C. pneumoniae*.

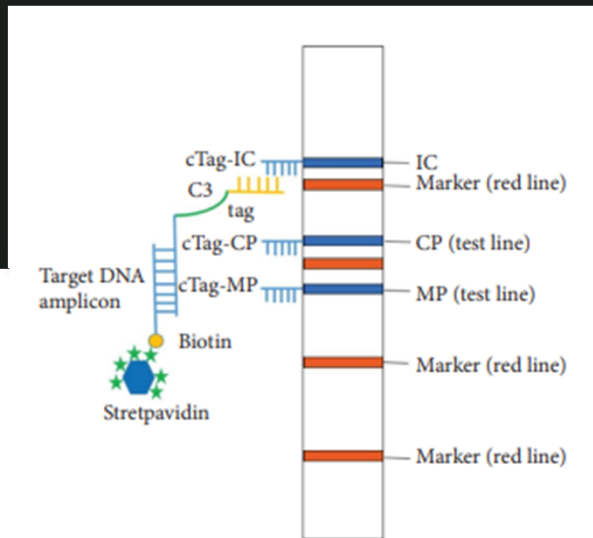
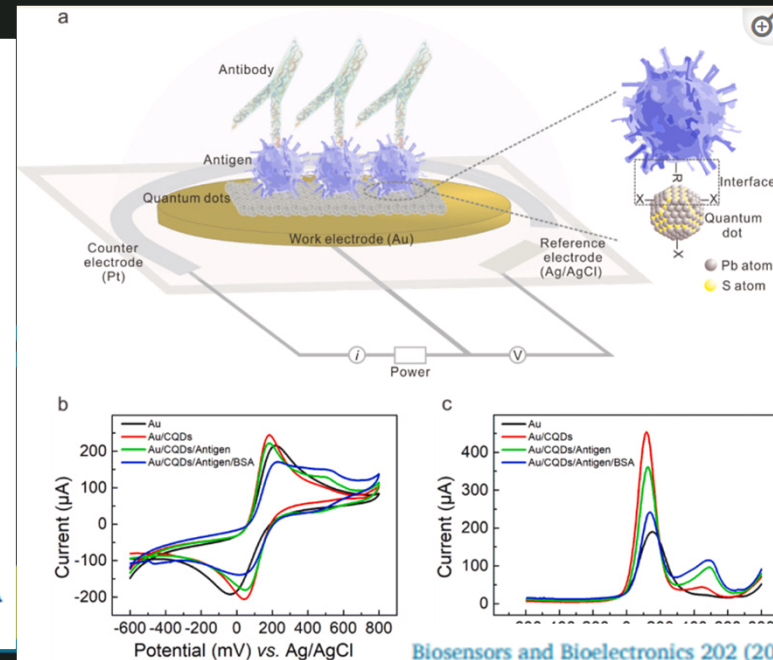


FIGURE 1: The schematic diagram of multiplex PCR-dipstick DNA chromatography.

Protein biosensor employing colloidal quantum dots-modified electrode

- recognize the specific binding reaction between antigen and antibody and then transduce it into significant electrical current.
- correlation coefficient of 93.8% compared to enzyme-linked immunosorbent assay (ELISA)
- Accuracy >90%
- < 1 min by handheld testing system prototype



Real time monitoring of POCT samples, critical results handling, quality control



Real time monitor of air quality

2023-04-18 09:41:31

全院综合概括

全院空气质量综合指数



全院感控风险指数分析



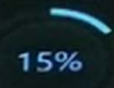
水体的物

物理区域感控

物理区域感控

智慧森林科室

全院智慧森林科室覆盖率



覆盖科室数量 24个

科室空气质量综合指数

1	心内二科	31	6	产科	40
2	检验医学部	32	7	神经内科	41
3	发热门诊	32	8	ICU科	42
4	生殖医学中心	32	9	病理科	47
5	消毒供应室	33	10	新生儿科	71

绿色节能

累计智能动态净化消毒 738338次

累计节约能耗 247263 kWh

相当于 105 个中国家庭一年用电量

553 CFU/m³

未检出

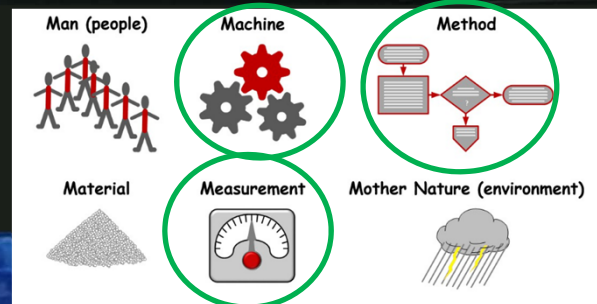
2463 个/col

PM2.5 26

PM10 580

TVOC 1443

相对湿度 25



CFU/m³ SARS-CoV2

E coli

C诊区——空气质量监测数据

PM2.5指数 37.84 ug/m³

PM10指数	实际温度	二氧化碳浓度
40.74	21.4	803.79
标准值 150ug/m ³	标准值 26°C	标准值 800ppm

设备开启状态监测

设备开启时长统计

区域	A区	B区	C区	D区	VIP区	大厅	一次候诊区
紫外线消毒模块	91%	88%	83%	95%	60%	100%	100%
光等离子杀菌模块	91%	88%	83%	95%	60%	100%	100%
静电除尘模块	91%	88%	83%	95%	60%	100%	100%

消杀效果监测报告

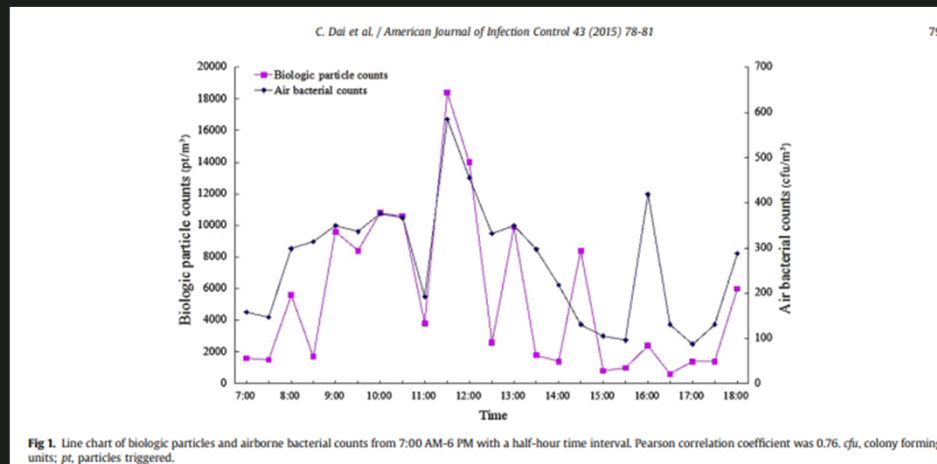
大肠杆菌

Real time monitor microbial aerosols

Fluorescent biologic particle

SARS-CoV2

Nature Communications | (2023)14:3692



- Laser-induced fluorescence to biologic particle (NADH, NADPH and flavins)
- Pearson correlation coefficient 0.76

At 0.65V, tyrosine in S protein oxidized & detected by MIE as peak oxidation current

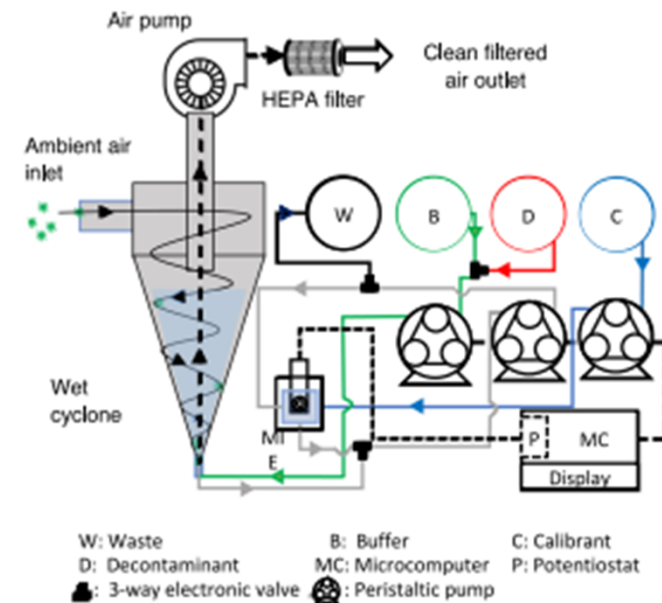
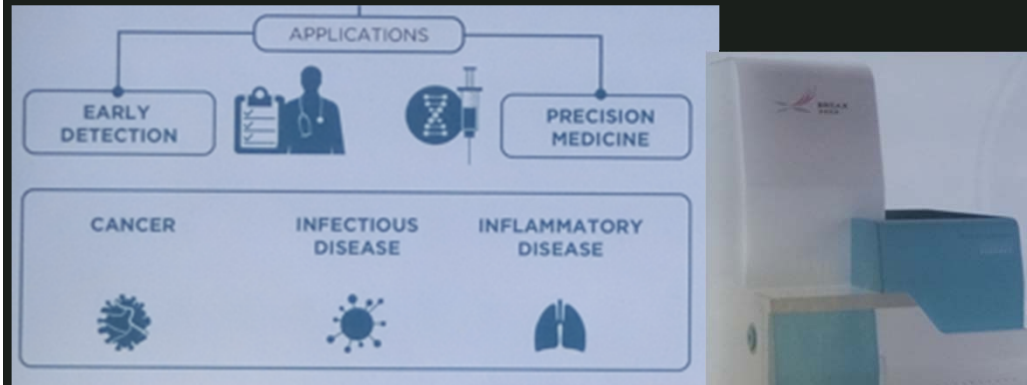


Fig. 1 | The layout of the pAQ monitor. a pAQ monitor schematic showing the wet cyclone PILS coupled with the MIE detection unit comprising a submerged MIE

- 5 min time resolution
- Nanobody (against spike protein)-based ultrasensitive micro-immunoelectrode (MIE) biosensor
- Sensitivity 77-83%, LOD 7-35 RNA copies/m³

American Journal of Infection Control 43 (2015) 78-81

Volatile Organic compounds



- Reflect **metabolites** of the infecting pathogen or pathogen-induced **host responses** or a combination of
- **exhaled-breath samples** are easy to collect
- gas-chromatography and mass-spectrometry (GCMS): analyzing individual compounds vs
- electronic nose (eNose) with pattern-recognition of chemical compounds using multivariate analysis (metal-oxide sensors with changes in conductivity)
- for noninvasive detection and monitoring of infectious diseases.

TABLE 4 Summary of published studies regarding the diagnostic performance of VOC profiles in detecting infectious diseases

Pathogen and disease	Sample source	VOC biomarker (no. of VOCs) ^a	No. of patients ^d			Sensitivity/specificity (%)
			DPG	ODG	HCG	
<i>Mycobacterium tuberculosis</i>						
TB	Breath	Profile (14)	23 ^b	19	59	96/79
Active TB	Breath	Profile (10)	226 ^c			84/65
Active TB	Breath	Profile (8)	130		121	72/72
TB	Breath	Profile (7)	50 ^b		50	72/86
			21 ^b	50		62/84
<i>Pseudomonas aeruginosa</i>						
Lung infection in patients with CF	Breath	Profile (21)	24		29	89/77
	Breath	Profile (14)	48		57	100/100
CF and non-CF bronchiectasis	Sputum	Profile (17)	32	28	12	91/88

^a Numbers in parentheses indicate the number of discriminatory VOCs.

^b TB culture positive.

^c Suspected TB.

^d DPG, disease patient group; ODG, other diseases group; HCG, healthy control group.

Clinical Microbiology Reviews p. 462–475

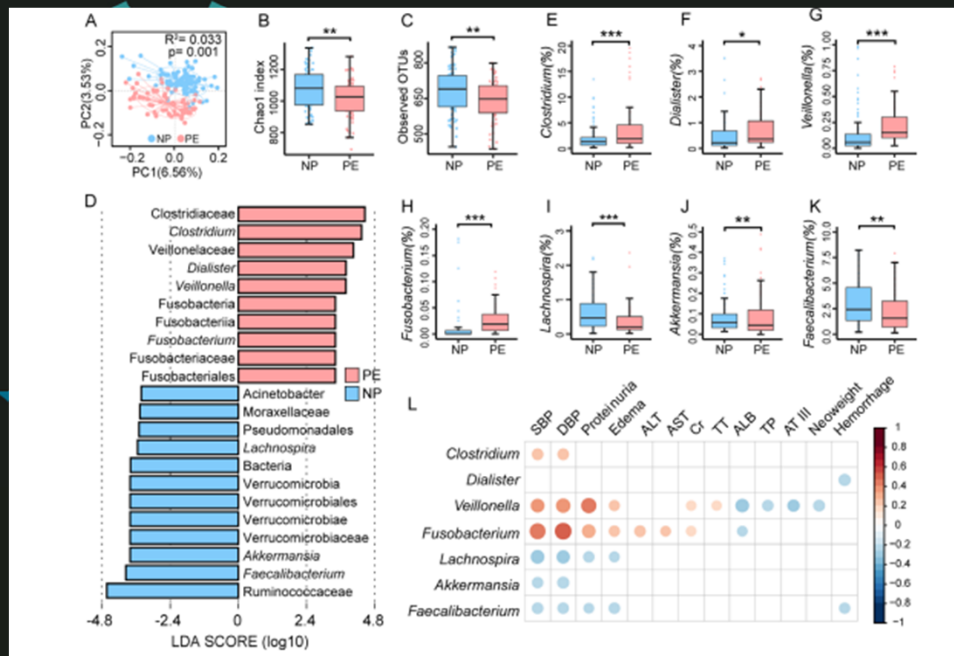
July 2013 Volume 26 Number 3

Studies, y	Annotation	True Positive (TP)	False Negative (FN)	False Positive (FP)	True Negative (TN)	Total Sample	Sensitivity (Sn; %)	Specificity (Sp; %)
Wintjens et al. 2020	N/A	49	8	75	87	219	86	53.7
Berna et al 2020	N/A	10	0	5	10	25	100	66.6
Grassin-Delyle et al 2020	N/A	25	3	1	11	40	90	94
Vries et al 2020	Validation Set	871	0	7	26	904	100	78.8
	Replication Set	1711	7	46	184	1948	99.6	80
	Asymptomatic Set	689	15	11	39	754	97.9	78
Ruszkiewicz et al 2020	Edinburgh Set	17	4	3	9	33	81	75
	Dortmunc Set	9	1	11	44	65	90	80
Shan et al 2020	COVID-19 vs Control Testing Set	11	0	7	11	29	100	61.1
	COVID-19 vs Lung Infection Testing Set	12	0	1	9	22	100	90

Gut Microbiome research – the paradigm shift

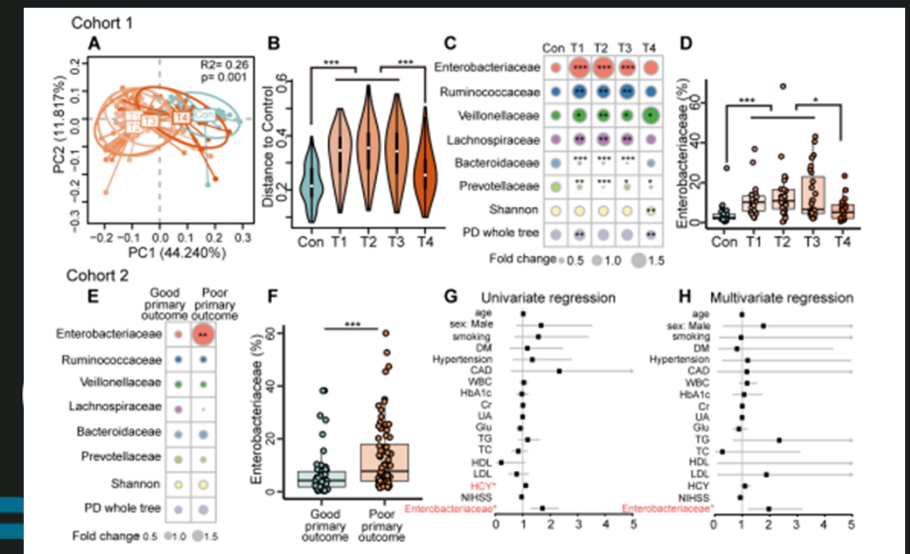
Gut dysbiosis induces the development of pre-eclampsia through bacterial translocation

Chen X, et al. *Gut* 2020;69:513–522. doi:10.1136/gutjnl-2019-319101



Rapid gut dysbiosis induced by stroke exacerbates brain infarction in turn

Xu K, et al. *Gut* 2021;0:1–9. doi:10.1136/gutjnl-2020-323263



Replicate the same result in mice models by FMT

